MEMBRANES AND BIOENERGETICS:

Characterization of the FET4 Protein of Yeast: EVIDENCE FOR A DIRECT ROLE IN THE TRANSPORT OF IRON

David Dix, Jamie Bridgham, Margaret Broderius and David Eide

J. Biol. Chem. 1997, 272:11770-11777.
doi: 10.1074/jbc.272.18.11770

THE JOURNAL OF BIOLOGICAL CHEMISTRY
Vol. 272, No. 18, Issue of May 2, pp. 11770–11777, 1997
Printed in U.S.A.

Characterization of the FET4 Protein of Yeast

EVIDENCE FOR A DIRECT ROLE IN THE TRANSPORT OF IRON*

(Received for publication, May 13, 1996, and in revised form, February 25, 1997)

David Dix, Jamie Bridgham, Margaret Broderius, and David Eide‡

From the Department of Biochemistry and Molecular Biology, University of Minnesota, Duluth, Minnesota 55812

The low affinity Fe^{2+} uptake system of *Saccharomyces cerevisiae* requires the *FET4* gene. In this report, we present evidence that *FET4* encodes the Fe^{2+} transporter protein of this system. Antibodies prepared against FET4 detected two distinct proteins with molecular masses of 63 and 68 kDa. *In vitro* synthesis of FET4 suggested that the 68-kDa form is the primary translation product, and the 63-kDa form may be generated by proteolytic cleavage of the full-length protein. Consistent with its role as an Fe^{2+} transporter, FET4 is an integral membrane protein present in the plasma membrane. The level of FET4 closely correlated with uptake activity over a broad range of expression levels and is itself regulated by iron. Furthermore, mutations in *FET4* can alter the kinetic properties of the low affinity uptake system, suggesting a direct interaction between FET4 and its Fe^{2+} substrate. Mutations affecting potential Fe^{2+} ligands located in the predicted transmembrane domains of FET4 significantly altered the apparent K_m and/or V_{max} of the low affinity system. These mutations may identify residues involved in Fe^{2+} binding during transport.

In many organisms, iron uptake is a two-step process in which extracellular Fe^{3+} is reduced to the more soluble Fe^{2+} form by plasma membrane Fe^{3+} reductases. The Fe^{2+} product is then taken up by Fe^{2+}-specific transport systems. This strategy of iron uptake is found in the yeast *Saccharomyces cerevisiae* (1–3), some bacteria (4, 5), other fungi (6, 7), and many plant species (8, 9). Mammalian cells may use a similar mechanism for uptake of iron across the mucosal membrane of the intestine (10–12) and for the uptake of free iron in blood plasma (13, 14). Mammalian cells acquire most of their iron from transferrin. Fe^{3+}-transferrin complexes bind to transferrin receptors on the cell surface. These receptor-ligand complexes are endocytosed to an endosomal compartment; the iron is dissociated and then transported across the endosomal membrane. Some studies have suggested that transferrin-delivered Fe^{3+} is reduced to Fe^{2+} in the endosome and transported into the cytoplasm by Fe^{2+}-specific transporters (15–17). Clearly, Fe^{2+} transporters play a prominent role in iron acquisition by a wide variety of organisms.

In *S. cerevisiae*, extracellular Fe^{3+} is reduced to Fe^{2+} by the plasma membrane Fe^{3+} reductases encoded by the *FRE1* and *FRE2* genes (18, 19). The Fe^{2+} product is then taken up by either of two transport systems. One system has a high affinity for iron (apparent K_m of 0.15 μM), is necessary for iron-limited growth, and requires the products of the *FET3* and *FTR1* genes for activity (20–23). The high affinity system is induced in iron-limited cells, and its components are transcriptionally regulated by the product of the *AFT1* gene (24). AFT1 is an iron-responsive DNA binding protein that activates transcription of the target promoters to which it binds (25).

Iron-replete yeast cells obtain iron through a second, low affinity uptake system with an apparent K_m of 30 μM. This system requires the *FET4* gene for activity. Our previous results suggested that FET4 is the low affinity Fe^{2+} transporter (26). First, overexpression of the *FET4* gene increased activity of an iron uptake system that was indistinguishable from the low affinity system. Second, disruption of the *FET4* gene eliminated low affinity uptake activity but did not diminish high affinity activity. Finally, the sequence of the *FET4* gene suggested that its product is a transporter protein. The predicted FET4 amino acid sequence is 552 residues in length and contains over 50% hydrophobic amino acids. Many of these hydrophobic residues are arranged in six regions that may be transmembrane domains. FET4 has no homology to any known protein including FTR1, the *feoB* Fe^{2+} transporter of *Escherichia coli* (27), and the *IRT1* Fe^{2+} transporter from *Arabidopsis thaliana* (28). Therefore, while the hydrophobic character of FET4 suggested that it is a transporter, we could not rule out other models of FET4 function. The central goal of the experiments described in this report was to further test the hypothesis that *FET4* encodes the Fe^{2+} transporter of the low affinity system.

EXPERIMENTAL PROCEDURES

Strains and Culture Methods—Yeast strains used were *DY1457* (*MATα ade6 can1 his3 leu2 trp1 ura3*), DEY1394 (*MATα ade6 can1 his3 leu2 trp1 ura3 fet3-2::HIS3*), DEY1422 (*MATa can1 his3 leu2 trp1 ura3 fet4-1::LEU2*), DEY1446 (*MATa can1 his3 leu2 ura3 fet4-1::LEU2 trp1::*YIpGAL1-FET4), DDY4 (*MATa ade6 can1 his3 leu2 trp1 ura3 fet3-2::HIS3 fet4–1::LEU2*), DEY1514 T1 (*MATa/MATα ade2/+ ade6/+ can1/can1 his3/his3 leu2/leu2 trp1/trp1::YIpGAL1-FET4 ura3/ura3*), and DEY1515 (*MATa/MATα ade2/+ can1/can1 his3/his3 leu2/leu2 trp1/trp1 ura3/ura3 fet4-1::LEU2/fet4-1::LEU2*). Cells were grown in 1% yeast extract, 2% peptone (YP) or synthetic defined (SD) medium (6.7 g/liter yeast nitrogen base) supplemented with any necessary auxotrophic requirements and either 2% glucose or 2% galactose. Cells were also grown in a modified iron-limited medium (LIM, Ref. 29) prepared without EDTA (*i.e.* LIM-EDTA) and supplemented with $FeCl_3$ to the stated concentrations. LIM-EDTA is iron limiting for growth of *fet3* mutant strains when supplemented with less than 10 μM $FeCl_3$ (data not shown) because of its high concentration (20 mM) of citrate, an iron-binding chelator. Yeast and *E. coli* transformations were performed using standard methods (30, 31).

Preparation of FET4-specific Antisera—The locations of potential transmembrane domains and the orientation of FET4 were predicted using TOP-PREDII software (32). Three segments of the FET4 protein, *i.e.* amino acids 1–60 (pGEMEX-N), 120–220 (pGEMEX-L1), and 410–460 (pGEMEX-L5), were selected as antigens. DNA fragments corre-

* This work was supported by Grant GM-48139 from the National Institutes of Health and the National Science Foundation Grant MCB-9405200. The costs of publication of this article were defrayed in part by the payment of page charges. This article must therefore be hereby marked "*advertisement*" in accordance with 18 U.S.C. Section 1734 solely to indicate this fact.

‡ To whom correspondence should be addressed. Present address: Dept. of Food Science and Human Nutrition, University of Missouri, Columbia, MO 65211. Tel.: 573-882-9686; Fax: 573-882-0185; E-mail: deide@showme.missouri.edu.

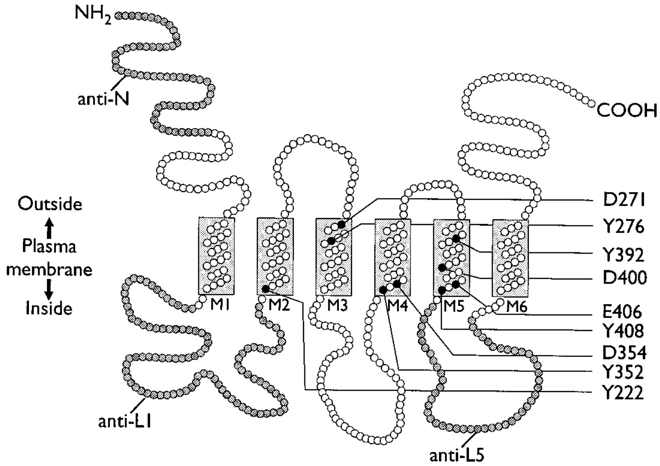

FIG. 1. **A model of FET4 membrane topology.** Transmembrane domains M1 through M6 are depicted as *rectangles*, and individual amino acid residues are indicated by the *circles*. Segments of the protein used in antibody preparation are shaded in *gray*. Mutated residues are *filled* and labeled using the single-letter amino acid code followed by the number of their position in the primary sequence.

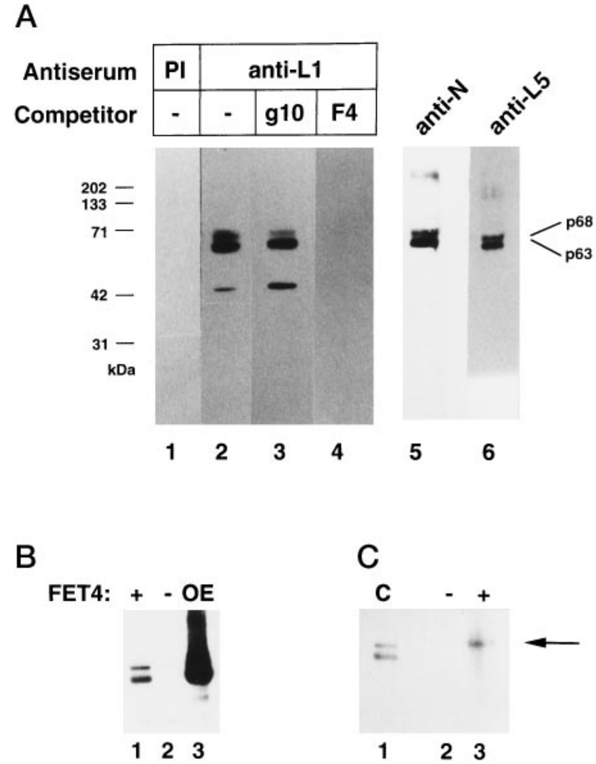

FIG. 2. **Detection of FET4.** *A*, immunoblots of total cell homogenates (10 μg of protein/lane) fractionated by SDS-polyacrylamide gel electrophoresis (10% acrylamide). Samples were prepared from *FET4*-overexpressing cells (*i.e.* DEY1446 cells grown on YP galactose medium). Blots were probed with either preimmune serum (*PI*) or the affinity purified anti-FET4 antibodies anti-L1, −N, and −L5. Where indicated, the primary antibody was preincubated with 10 μg of purified gene 10 protein (*g10*) or the L1-gene 10 fusion protein (*F4*) for 1 h prior to incubation with the blot. *B*, particulate/membrane proteins from YP glucose-grown wild type (DY1457, +) and *fet4* (DEY1422, −) cells and *FET4*-overexpressing cells (DEY1446, OE) grown on YP galactose medium were analyzed by immunoblotting. *C*, *in vitro* transcription/translation of FET4. Total cell homogenate isolated from *FET4*-overexpressing DEY1446 (10 μg of protein; *C*), or the product of a coupled *in vitro* transcription/translation reaction (25 μl) containing either the vector (pLO-LB, −) or a *FET4*-expressing plasmid (pLO-LBFET4, +) were analyzed by immunoblotting. The *arrow* indicates FET4 generated in the *in vitro* reaction.

sponding to these regions were obtained using polymerase chain reaction primers with appropriate restriction sites added to their 5′ ends and cloned into pGEMEX-1 (Promega). In-frame cloning of these inserts into this vector produced genes in which the bacteriophage gene 10 protein is fused to the FET4 peptide. The fusion proteins were expressed in *E. coli* strain BL21 (DE3) pLysS as described by Studier *et al.* (33). Cells were harvested by centrifugation, boiled in SDS sample buffer, and centrifuged at 12,000 × *g* for 1 min to remove cell debris. The supernatant was fractionated by SDS-polyacrylamide gel electrophoresis in a Bio-Rad 491 Prep Cell. Rabbits were injected subcutaneously with 100 μg of semi-purified fusion protein in adjuvant. Anti-FET4 antibodies were affinity purified against their corresponding gene 10-FET4 fusion protein by column chromatography (34).

In Vitro Synthesis of FET4—A *Bam*HI-*Sac*I fragment bearing the *FET4* open reading frame was generated by polymerase chain reaction and inserted into pLO-LB (L. Opresko, University of Utah) to generate pLO-LBFET4. *In vitro* transcription/translation was performed using the TnT system (Promega).

Preparation of Protein Extracts and Fractionation on Sucrose Density Gradients—Cells were grown to exponential phase (100 ml, A_{600} of 2–4), spheroplasts were prepared (35), resuspended in 10 ml of 0.6 M mannitol, 20 mM HEPES-KOH, pH 7.4, 1 mM EDTA, 1 mM phenylmethylsulfonyl fluoride, 1 mM pepstatin A, and disrupted in a Dounce homogenizer. Total cell homogenates were obtained by centrifuging these samples at 3000 × *g* for 5 min at 4 °C and discarding the pellet of unbroken cells. The homogenates were then centrifuged at 123,000 × *g* for 30 min at 4 °C to yield the soluble (supernatant) and particulate/membrane (pellet) fractions. Sucrose density gradient fractionation was performed as described previously (36). One ml of total cell homogenate (approximately 1 mg of protein) was loaded onto the top of linear sucrose gradients (20–55% w/w). The gradients were centrifuged for 16 h at 110,000 × *g* in an SW41 rotor at 4 °C. Fractions (700 μl each) were collected sequentially from the top of the gradients beginning with fraction 1.

Immunoblot Analysis—Immunoblots were performed as described previously (34) using primary antibodies specific to FET4, PMA1 (37), HMG1 (38), VPH1 (Molecular Probes, Inc.) and OMP2 (G. Schatz, Basel). Unless stated otherwise, anti-L1 was used for detection of FET4. Horseradish peroxidase-conjugated goat anti-rabbit antibody (Pierce) was used as the secondary antibody; protein-antibody complexes were detected with enhanced chemiluminescence (Amersham Corp.). Densitometric scanning was performed using a CCD camera and IMAGE 1.44 software (National Institutes of Health).

Indirect Immunofluorescence Microscopy—Indirect immunofluorescence microscopy was performed essentially as described by Pringle *et al.* (39) with the following modifications. Cells were fixed in 10 volumes of cold methanol (−20 °C) for 30 min. Fixed cells were treated with glusulase to remove the cell wall and bound to polylysine-treated coverslips. Primary antibody staining was performed by incubating the cells with affinity-purified anti-FET4 antibodies (1:200 dilution in phosphate-buffered saline) at room temperature for 16 h. Following washing of the cells, goat anti-rabbit IgG secondary antibody (Pierce) was applied (1:200 dilution in phosphate-buffered saline), and the cells were incubated at 37 °C for 1 h. This was followed by incubation at 37 °C for 1 h with streptavidin-conjugated fluorescein isothiocyanate (Zymed) diluted 1:400 in phosphate-buffered saline.

Plasmids and Site-directed Mutagenesis—YIpGAL1-FET4 was constructed by inserting the 2.7-kilobase *Kpn*I-*Sac*I fragment from pCB1 (26) into pRS304 (40). This plasmid was digested with *Xba*I and transformed into DEY1422 to generate DEY1446 (41). Plasmid pCB2 is a derivative of pCB1 that contains a 66-base pair deletion in the *FET4* 5′-untranslated region. YIpGF4d1 was constructed by cloning the *GAL1-FET4 Kpn*I-*Not*I fragment of pCB2 into pRS304. Mutations were generated in YIpGF4d1 by site-directed mutagenesis using the Transformer system (CLONTECH) and verified by DNA sequencing. The resulting plasmids were linearized by digestion with *Xba*I and transformed into DDY4. Trp^+ colonies were isolated and confirmed to contain the *GAL1-FET4* fusion gene by polymerase chain reaction.

Fe^{2+} Uptake and Fe^{3+} Reductase Assays—The Fe^{2+} uptake and Fe^{3+} reductase assays were performed at 30 °C as described previously (3) except that ^{55}Fe was substituted for ^{59}Fe, and radioactivity was measured by liquid scintillation counting. Iron accumulation by wild type and mutant cells at 30 °C was found to be linear over the entire time of the uptake rate determination. ^{55}Fe accumulation due to cell surface binding was estimated by incubating parallel samples at 0 °C for the same period as the assay. These values were then subtracted from the 30 °C samples before calculation of uptake rates. The 0 °C values, which never exceeded 5% of the 30 °C samples, were similar to the level of iron

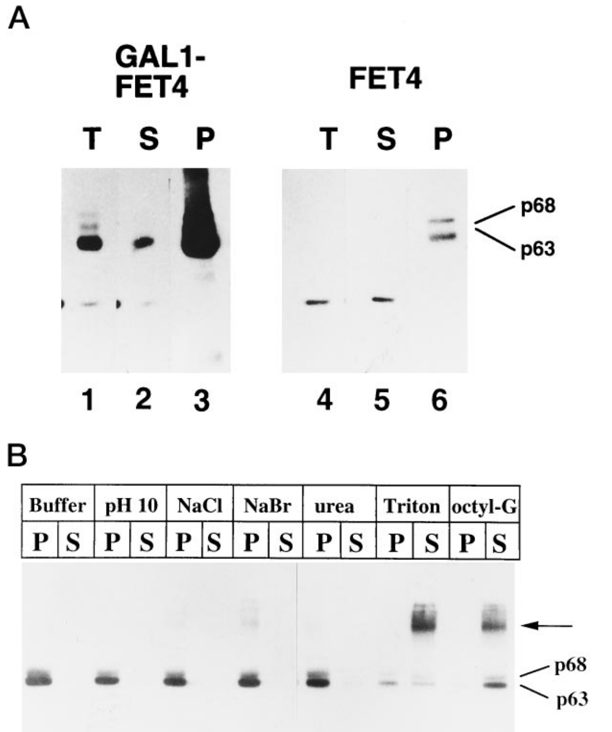

FIG. 3. **FET4 is an integral membrane protein.** *A*, *FET4*-overexpressing cells (DEY1446, GAL1-FET4) and wild type cells (DY1457, FET4) were grown to exponential phase in YP galactose and YP glucose, respectively. Total cell homogenates (*T*) were separated into soluble (*S*) and particulate/membrane (*P*) fractions by ultracentrifugation. These samples (10 μg of protein/lane) were then analyzed by immunoblotting. *B*, a particulate/membrane fraction from *FET4*-overexpressing cells was resuspended in 0.4 M sucrose, 25 mM imidazole, 200 mM EDTA, pH 6.8 (SIE) plus protease inhibitors. This sample was divided into 1-ml aliquots (0.4 mg of protein each) and centrifuged for 45 min at 65,000 × *g* at 4 °C. Pellets were resuspended in 0.2 ml of SIE (Buffer), 10 mM Na_2CO_3, pH 10.0, or SIE supplemented with either 1 M NaCl, 0.8 M NaBr, 2.5 M urea, 1% Triton X-100, or 1% *n*-octyl-β-D-glucopyranoside. Samples were held on ice for 30 min and then centrifuged at 65,000 × *g* at 4 °C for 45 min, and pellet (*P*) (resuspended in 0.2 ml of SIE) and supernatant (*S*) fractions were analyzed by immunoblotting. Equal volumes of each sample (20 μl) were loaded per lane. The slower migrating FET4 protein is indicated by the *arrow*.

accumulation observed with a *fet3 fet4* mutant at 30 °C indicating that this was an appropriate method for measuring cell surface iron binding. Determinations of apparent K_m and V_{max} values were made by fitting the data directly to theoretical curves using KINETASYST software (Intellikinetics, Princeton, NJ).

RESULTS

Immunological Detection of the FET4 Protein—Based on the "positive-inside" rule (42), a model was devised describing the topology of FET4 in a lipid bilayer membrane (Fig. 1). Three hydrophilic regions of the protein were selected for use as antigens to generate antibodies against FET4. These regions were the amino-terminal 60 amino acids (anti-N), 101 amino acids located between transmembrane domains 1 and 2 (anti-L1), and 51 amino acids located between transmembrane domains 5 and 6 (anti-L5). These portions of FET4 were expressed in *E. coli* as fusions to the phage T7 gene 10 protein and purified. The fusion proteins were then injected into rabbits and affinity-purified antisera were prepared.

On immunoblots, while the preimmune serum did not detect any proteins in total cell homogenates (Fig. 2*A*, *lane 1*), anti-L1 antibody detected three proteins of 68 kDa ("p68"), 63 kDa ("p63"), and 46 kDa ("p46") molecular mass (Fig. 2*A*, *lane 2*). The predicted molecular mass of FET4 is 63 kDa. Detection of p68, p63, and p46 could be blocked by preincubation of the antibody with the gene 10-FET4 fusion protein but not by preincubation with gene 10 protein alone (Fig. 2*A*, *lanes 3* and *4*). Thus, these three proteins are detected by antibodies that recognize the FET4 portion of the fusion protein. Further ex-

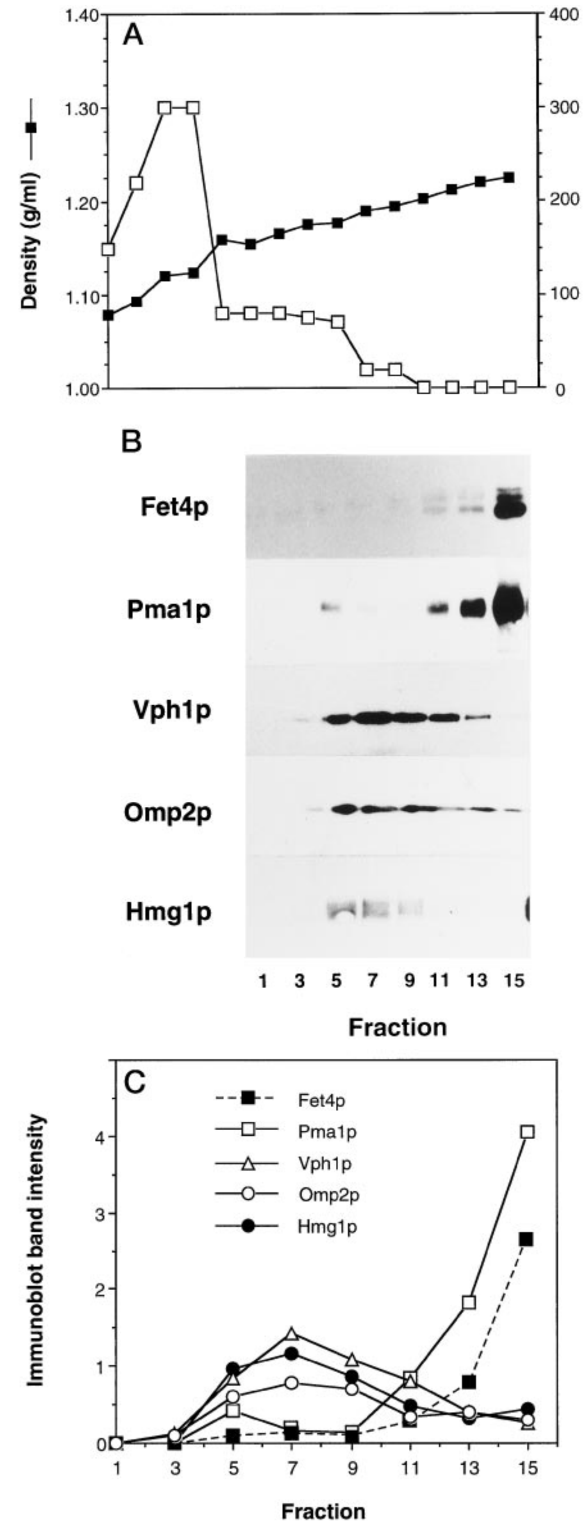

FIG. 4. **Fractionation of FET4 on sucrose density gradients.** A total cell homogenate prepared from *fet3* (DEY1394) cells grown to exponential phase in LIM-EDTA supplemented with 10 μM $FeCl_3$ was fractionated on a 20–55% (w/w) sucrose gradient. *A*, fractions were assayed for protein content and sucrose density. *B*, equal volumes (20 μl) of the odd-numbered fractions were analyzed by immunoblotting with indicated antibodies. *C*, the signal intensities of the immunoblot bands in *B* were measured by densitometry (arbitrary units).

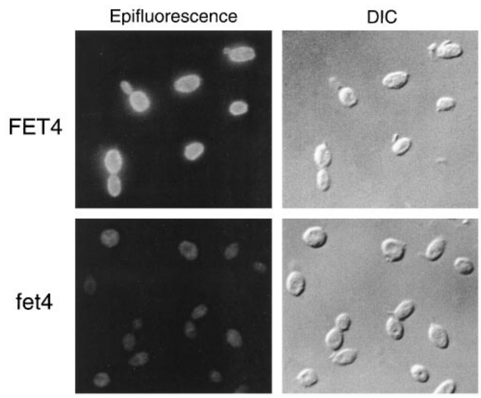

FIG. 5. **Indirect immunofluorescence microscopy of FET4.** Cells overexpressing the *FET4* gene (DEY1514T1, FET4) or mutant in the *fet4* gene (DEY1515, fet4) were fixed, treated with affinity purified anti-L1 antibodies, stained with secondary goat anti-rabbit IgG and streptavidin-conjugated fluorescein isothiocyanate, and visualized by epifluorescence and by DIC optics.

periments demonstrated that both p63 and p68 are products of the *FET4* gene, whereas p46 is encoded by another gene. First, the two other anti-FET4 antibodies, anti-N and anti-L5, detected p68 and p63 but not p46 (Fig. 2*A*, *lane 5* and *6*). Furthermore, p68 and p63 levels were altered by overexpression and deletion of the *FET4* gene; p68 and p63 levels were low in wild type cells, undetectable in *fet4* mutant cells, and very high in cells overexpressing the *FET4* gene from the *GAL1* promoter (Fig. 2*B*). The level of p46 was unaffected by differential *FET4* expression.

What is the relationship between the p68 and p63 forms of FET4? Neither p68 nor p63 is *N*-glycosylated or phosphorylated; no change in electrophoretic mobility was observed when membrane proteins were treated with endoglycosidase H, peptide *N*-glycosidase F, or alkaline phosphatase (data not shown). To determine which form was the primary translation product, we synthesized FET4 *in vitro* (Fig. 2*C*). Although no protein product was detected in a control reaction with the vector alone, a *FET4* expression plasmid directed the synthesis of a FET4 protein with the same electrophoretic mobility as p68. These results suggested that p68 is the primary translation product of the *FET4* gene and p63 is an altered form generated, perhaps, by proteolytic cleavage of p68. This proteolysis probably occurs *in vivo* because it was not prevented by the addition of protease inhibitors to the homogenization buffers nor was it prevented when proteins were prepared from a strain, BJ2168, that is defective for several vacuolar proteases (43). The physiological significance of this modification is unclear; the abundance of p63 relative to p68 was variable and did not correlate with the level of iron in the growth medium, the level of *FET4* expression, or the carbon source on which the cells were grown (data not shown).

FET4 Is an Integral Membrane Protein—Cellular proteins were separated into soluble and particulate/membrane fractions, and these fractions were examined for the presence of FET4 by immunoblotting (Fig. 3*A*). In either *FET4* overexpressing (*lanes 1–3*) or wild type (*lanes 4–6*) cells, both p63 and p68 were highly enriched in the particulate/membrane fraction. A small amount of the p63 form was also found in the soluble fraction in *FET4*-overexpressing cells. This may be due to the presence of p63 in small vesicles that sediment slowly during ultracentrifugation. The p46 protein was found only in the soluble protein fraction.

The enrichment of FET4 in the particulate/membrane fraction suggested that this protein was associated with membranes. When this fraction was treated with high pH, NaCl,

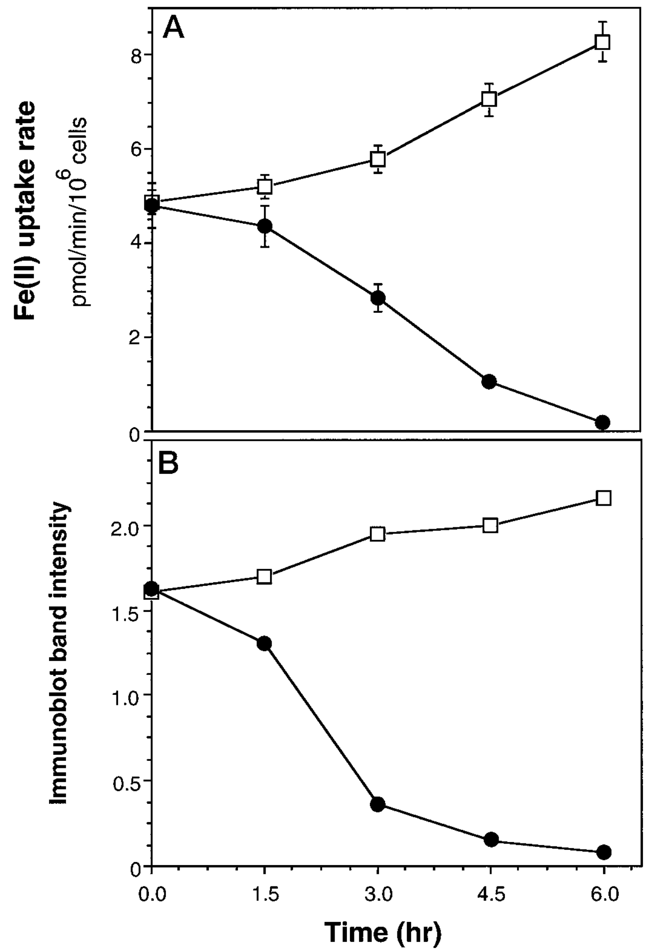

FIG. 6. **Correlation between iron uptake activity and FET4 levels.** FET4-overexpressing cells (DEY1446) were grown to exponential phase in YP galactose. These cells were then divided into two cultures; glucose was added to one culture to a final concentration of 2% (*closed circles*) and not to the other culture (*open squares*). *A*, these cultures were incubated at 30 °C, and aliquots were removed at the indicated time points and assayed for Fe^{2+} uptake activity. The *error bars* indicate ±1 S.D. *B*, total cell homogenates were prepared from the cultures in *A* and analyzed by immunoblotting. Signal intensities of the immunoblot bands were measured by densitometry (arbitrary units).

NaBr, or urea, *i.e.* agents that disrupt protein-protein interactions (44), FET4 remained associated with the particulate/membrane fraction (Fig. 3*B*). Treatment with the detergents Triton X-100 and *n*-octyl-β-D-glucopyranoside released FET4 into the soluble fraction. These results indicate that FET4 is an integral membrane protein. Slower migrating forms of FET4 were observed in the detergent-solubilized fractions that may be dimeric FET4. Consistent with this hypothesis, the molecular mass of this complex was 130–140 kDa, *i.e.* twice the monomeric FET4 mass.

FET4 Is Found in the Plasma Membrane—The subcellular location of FET4 was first assessed by fractionation of cellular membranes on a 20–55% (w/w) sucrose gradient. The density of the isolated fractions increased linearly from 1.08 to 1.22 g/ml, and protein was most abundant in the lowest density fractions where soluble proteins are found (Fig. 4*A*). Equal volumes of alternate fractions were analyzed by immunoblotting for the presence of FET4 and several marker proteins specific to particular subcellular compartments (Fig. 4*B*), and these blots were quantitated by densitometric scanning (Fig. 4*C*). FET4 was most abundant in fraction 15 (*d* 1.22 g/ml; 55% sucrose). PMA1, the plasma membrane marker protein, was also most abundant in fraction 15 as was the product of an epitope-tagged

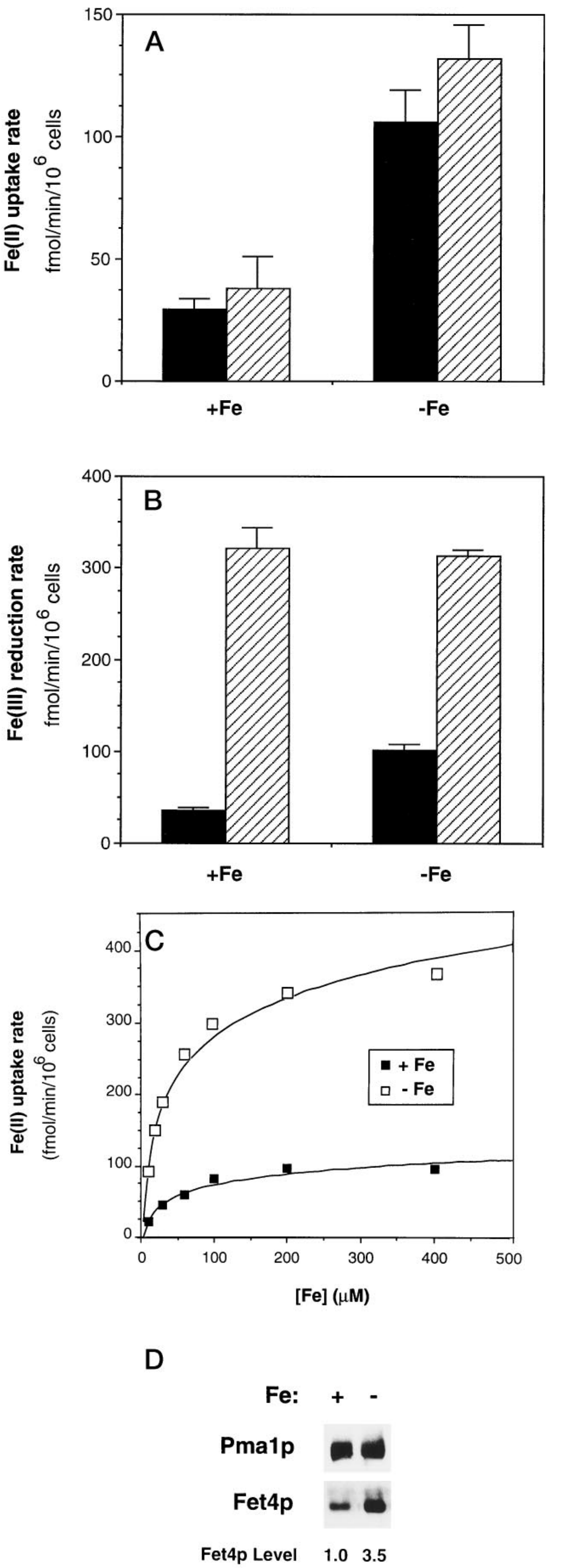

FIG. 7. **Regulation of low affinity uptake and FET4 levels by iron.** *fet3* cells (DEY1394, *filled columns*) or *fet3* cells transformed with the *AFT1–1^up* plasmid pT14 (*hatched columns*) were grown to exponential phase in LIM-EDTA supplemented with 1000 μM (+*Fe*) or 10 μM (−*Fe*) $FeCl_3$. Cells were harvested and assayed for Fe^{2+} uptake activity (*A*) and Fe^{3+} reductase activity (*B*). Shown are the results of a representative experiment, and each value was derived from four samples. The *error bars* represent 1 S.D. *C*, kinetic analysis of Fe^{2+} uptake in iron-replete and iron-limited cells. DEY1394 was grown to exponential phase in LIM-EDTA supplemented with 1000 μM (+*Fe*, *closed squares*) or 10 μM (−*Fe*, *open squares*) $FeCl_3$. The data shown are the means of two separate experiments each performed in duplicate, and the standard deviation within each experiment was <10% of the mean. *D*, particulate/membrane fractions were prepared from DEY1394 cells grown as in *C* and analyzed by immunoblotting using anti-PMA1 and anti-FET4 antibodies. The intensities of the FET4 bands were measured by densitometry (arbitrary units).

CTR1 allele (data not shown). CTR1 is the high affinity copper transporter and has also been localized to the plasma membrane (45). The presence of PMA1, CTR1, and FET4 in the bottom fraction of the gradient was not due to protein aggregation. When fraction 15 was treated with *n*-octyl-β-D-glucopyranoside and reloaded onto a sucrose gradient, these proteins were found in the low density fractions (data not shown). Marker proteins specific for intracellular compartments, *i.e.* the vacuolar VPH1 protein, the mitochondrial OMP2 protein, and the endoplasmic reticulum HMG1 protein were most abundant in lower density fractions. In a similar experiment, a Golgi marker protein (dipeptidyl-aminopeptidase A) showed a distribution in the gradient like that of OMP2 (36). Thus, FET4 co-fractionated with plasma membranes in these gradients.

By indirect immunofluorescence microscopy, the FET4 protein could be visualized as a bright rim of fluorescence at the periphery of cells overexpressing the *FET4* gene (Fig. 5). Similar results were obtained with anti-N antibody (data not shown). In contrast, a *fet4* mutant strain did not show this peripheral staining. These results also indicate that FET4 is a plasma membrane protein. Attempts to detect FET4 when expressed at wild type levels were unsuccessful probably due to the protein's normally low level of synthesis (Fig. 2*B*).

Correlation of FET4 Levels, Low Affinity Uptake, and Regulation by Iron—*FET4* overexpression increased low affinity uptake activity, whereas disruption of the gene eliminated that activity (26). This correlation supported the hypothesis that *FET4* encodes the Fe^{2+} transporter of the low affinity system. To test this correlation more rigorously, we used the fusion gene in which *FET4* is expressed under the regulation of the *GAL1* promoter. Cells overexpressing *FET4* in galactose-containing medium were split into two cultures, and glucose was added to one culture to shut off expression of the *GAL1* promoter; *GAL1* promoter activity is reduced to less than 10% of the induced level within 5 min of glucose addition (46). Cells were harvested periodically and assayed for Fe^{2+} uptake activity (Fig. 6*A*) and FET4 levels (Fig. 6*B*). The activity of the low affinity system in untreated cells increased slightly as did the level of FET4. In glucose-treated cells, low affinity uptake decreased approximately 40-fold. FET4 levels declined to a similar degree, and its profile was almost superimposable with the loss of uptake activity. Thus, FET4 levels and uptake activity of the low affinity system closely correlated over a broad range of expression levels.

To determine if the low affinity system is iron-regulated, we measured this activity in iron-replete and iron-limited cells. A *fet3* mutant was used for this analysis to allow measurement of low affinity activity in the absence of the high affinity system. The low affinity system is iron-regulated; uptake activity increased approximately 3-fold in iron-limited cells (Fig. 7*A*). Fe^{3+} reductase activity was also induced approximately 3-fold in these cells, confirming that this medium was iron-limiting (Fig. 7*B*). To assess if AFT1 plays a role in this regulation, we

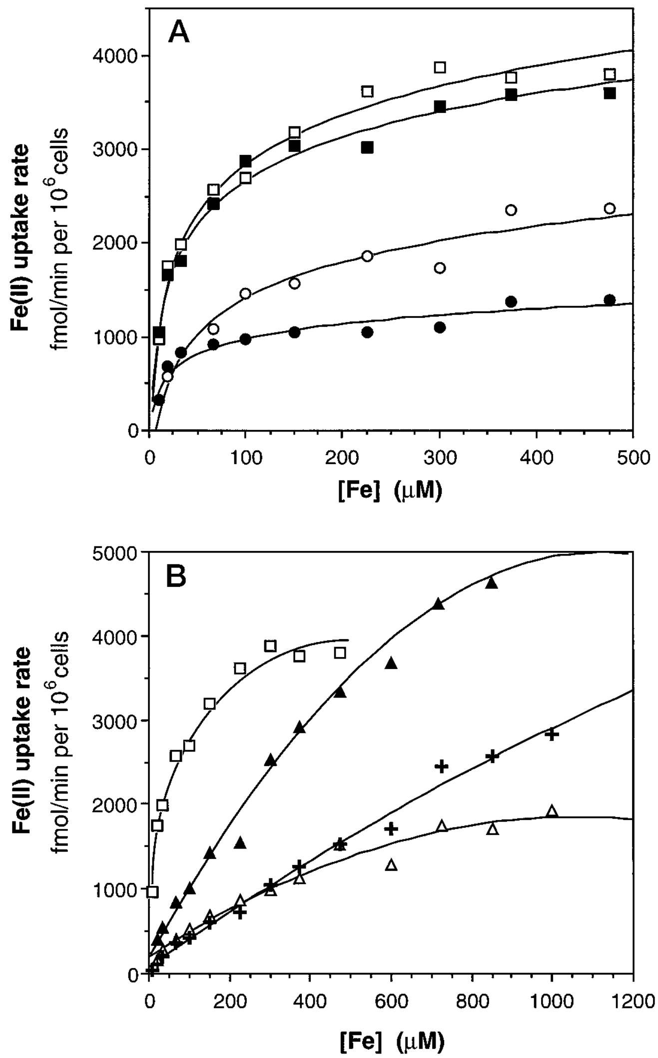

FIG. 8. **Kinetic analysis of wild type and mutant *FET4* alleles.** DDY4 cells expressing the indicated *FET4* allele from YIpGF4d1 were grown in YP galactose to exponential phase and assayed for Fe^{2+} uptake over a range of iron concentrations. The data shown are the means of four or more samples, and the standard deviation of each was <10% of the corresponding mean. The symbols used are: □, wild type; ■, Y222A; ○, Y392A; ●, Y408A; ▲, Y276A; △, Y352A; +, D271A.

measured uptake activity in a strain bearing the *AFT1-1*^{up} allele. *AFT1-1*^{up} causes constitutively induced expression from *AFT1*-responsive promoters (24). Activity of the low affinity system was not increased by the *AFT1-1*^{up} allele, whereas Fe^{3+} reductase activity was constitutively active in this strain. These results indicate that the low affinity activity is regulated in response to iron by a mechanism distinct from AFT1 transcriptional activation.

The increased uptake activity in response to iron limitation was caused by a change in V_{max}, whereas the apparent K_m was unaffected (Fig. 7*C*). The apparent K_m and V_{max} of iron-replete cells was 41 ± 7 μM Fe^{2+} and 110 ± 15 fmol/min/10^6 cells, respectively. In iron-limited cells, the apparent K_m was 33 ± 8 μM Fe^{2+}, and the V_{max} was 372 ± 27 fmol/min/10^6 cells. Immunoblots demonstrated that while the level of the PMA1 plasma membrane ATPase was unaffected by iron limitation, FET4 levels increased approximately 3-fold (Fig. 7*D*).

Characterization of FET4 Mutant Alleles—The experiments described above support the hypothesis that *FET4* encodes the low affinity transporter protein. The identification of mutations in *FET4* that alters intrinsic kinetic properties of the low affinity system also supports this hypothesis. Especially informative are mutations that alter the affinity (*i.e.* apparent K_m) of the system for Fe^{2+} because this parameter is determined by the direct interaction of the transporter with its substrate (47). We anticipated that critical ligands for Fe^{2+} binding would be located in or near the predicted transmembrane domains. Nine potential ligands were chosen for site-directed mutagenesis (Fig. 1) (see "Discussion"). In each case, the amino acid was replaced with an alanine residue because such mutations have been demonstrated to minimize structural alterations in the protein (48). The mutant alleles were expressed from the *GAL1* promoter in a *fet3 fet4* mutant strain and assayed for Fe^{2+} uptake.

TABLE I
Effects of FET4 alleles on low affinity Fe^{2+} uptake

The apparent K_m and V_{max} values were determined from the data in Fig. 8 and are the means (± 1 S.E.) of several replicates for each strain ($n \geq 4$). ND, no uptake activity detectable.

FET4 allele	K_m	V_{max}
	μM	*fmol/min/10^6 cells*
wild type	35 ± 5	4072 ± 156
Y222A	29 ± 4	3664 ± 116
Y392A	87 ± 20	2648 ± 195
Y408A	22 ± 7	1293 ± 73
D271A	≥1000	≥4000
Y276A	787 ± 137	8743 ± 912
Y352A	458 ± 93	2682 ± 251
D354A	ND	
D400A	ND	
E406A	ND	

The effects of these mutations on the concentration dependence of *FET4*-mediated Fe^{2+} uptake were determined (Fig. 8), and the apparent K_m and V_{max} values derived from these data are summarized in Table I. Two of the nine alleles, Y222A and Y408A, had little effect on the apparent K_m for Fe^{2+}. A third allele, Y392A, increased the K_m approximately 2.5-fold. Three other alleles increased the apparent K_m even higher. These increases ranged from 13-fold for Y352A to more than 30-fold for D271A. V_{max} values were also altered for several of these alleles, ranging from 30 to 200% of the wild type rates. No saturability of D271A-dependent uptake was observed in assays conducted with Fe^{2+} concentrations as high as 3 mM (data not shown), preventing an accurate determination of the V_{max} of this allele. Clearly, mutations in *FET4* can greatly alter the kinetic properties of the low affinity system.

Three mutations, D354A, D400A, and E406A, completely eliminated low affinity uptake activity. While D354A and D400A produced wild type levels of FET4, no protein was detected in the E406A-expressing strain (data not shown). Subcellular fractionation of proteins from D354A and D400A on sucrose density gradients indicated that these forms were properly localized to the plasma membrane (data not shown). When overexpressed in a wild type *FET4* strain, however, D354A and D400A were both found to be recessive.

DISCUSSION

The experiments described in this report test the hypothesis that FET4 is the Fe^{2+} transporter protein of the low affinity system. Consistent with this role, FET4 is an integral membrane protein and localized to the plasma membrane. Additional supporting evidence was provided by the close correlation between FET4 levels and uptake activity. This correlation was demonstrated in studies where the *FET4* gene was overexpressed under the control of the *GAL1* promoter as well as when it was expressed from its own promoter.

These experiments also indicated that the low affinity system is regulated by iron. The V_{max} of the low affinity uptake increased approximately 3-fold in iron-limited cells relative to iron-replete cells, and a similar degree of induction was observed for FET4 levels. Fe^{3+} reductase activity was also induced by iron limitation in these cells. Despite this similarity, FET4 and the Fe^{3+} reductase activity are probably not regulated by the same mechanism because they respond differently to the *AFT1-1^up^* allele. *AFT1* encodes a transcriptional activator that controls the expression of several iron-responsive genes including the Fe^{3+} reductase genes *FRE1* and *FRE2*. The *AFT1-1^up^* allele causes constitutive expression of all of the genes known to be regulated by this protein (24, 25). This allele had no effect on the regulation of the low affinity system, suggesting that an additional system of iron-responsive regulation exists in *S. cerevisiae*.

Strong evidence for the role of FET4 as an Fe^{2+} transporter was also obtained from characterizing mutations in the *FET4* gene. We hypothesized that if FET4 was the transporter, it would be possible to isolate mutant alleles of *FET4* that alter the kinetic properties of the low affinity system. Of particular interest were mutations that changed the affinity (*i.e.* apparent K_m) of the system for Fe^{2+} because this parameter is determined by the direct interaction of the transporter with its substrate. An examination of the amino acid sequence of FET4 did not reveal any obvious metal-binding motifs in the hydrophilic regions of the protein. Such motifs, which have been observed for other metal transporters such as CTR1 (45), CCC2 (21), FTR1 (23), and IRT1 (28), may be involved in substrate binding during transport. The observation that FET4 lacks such sequences suggested that initial binding of Fe^{2+} by this protein could be mediated by ligands located within the transmembrane domains.

Fe^{2+} is a borderline hard-soft Lewis acid, so potential ligands include oxygen-containing hard Lewis bases as well as sulfur-containing soft Lewis bases (49). Thus, each transmembrane domain contains several potential Fe^{2+} ligands. For this analysis, we mutagenized aspartate and glutamate residues and the "hydrophobic anion" (50) tyrosine. Aspartates and glutamates were chosen because their negative charge makes them likely candidates for interaction with a cationic substrate. Such amino acids have been implicated in substrate binding by other cation transporters. Based on an analysis similar to ours, the substrate-binding site of the sarcoplasmic reticulum Ca^{2+}-ATPase has been proposed to utilize three glutamates and an aspartate (51, 52). Furthermore, we considered the iron-binding protein ferritin as a paradigm for how an Fe^{2+} transporter might bind its substrate. Ferritin is a cytoplasmic protein that assembles into a hollow, spherical complex that is capable of taking up Fe^{2+}. This complex has an outer diameter of 130 Å and an inner diameter of 75 Å and the channels through which Fe^{2+} passes are lined with glutamates. These negatively charged amino acids, present in the consensus sequence RE(G/H)AE, have been implicated in the transport of iron into the protein shell of ferritin (53). Recently, glutamates in a similar sequence motif (REGLE) were found in a potential transmembrane domain of FTR1 and demonstrated to be critical for iron uptake by this permease (23). Although a similar motif is not found in FET4, these observations suggested that negatively charged residues may be important for FET4 Fe^{2+} binding.

Tyrosine residues in the potential transmembrane domains were also of interest because these residues can bind iron through interaction of the dipole moment of the electronegative oxygen in the hydroxyl group or through a cation-Π interaction involving the quadrupole moment of the aromatic ring. It was recently proposed that the relatively hydrophobic side chains of amino acids with quadrupole moments (*i.e.* tyrosine, phenylalanine, and tryptophan) would be well-suited to serve as cation ligands while embedded in the environment of a transmembrane domain (50). Furthermore, tyrosines have been proposed to play a role in the ion selectivity of voltage-gated K^+ channels like the Shaker channel of *Drosophila* (54).

Based on these criteria, nine amino acids were chosen for mutagenesis. Measurable V_{max} values in this collection of mutants ranged from 30 to 200% of wild type rates. Three alleles, D271A, Y276A, and Y352A, had 13- to >30-fold higher apparent K_m values than the wild type. These effects strongly suggest that there is a direct interaction between FET4 and the substrate of the low affinity system. It is very possible that one or more of these residues are ligands for Fe^{2+} binding during transport. It seems unlikely that all three amino acids are ligands given that D271A and Y276A are predicted to be near the outer surface of the plasma membrane and Y352A is predicted to be near the inner surface of the membrane. Reconciling these data in terms of a single Fe^{2+} binding site will require a careful analysis of the membrane topology of FET4.

Acknowledgments—We thank Jon Holy for assistance with the indirect immunofluorescence microscopy, Lee Opresko for pLO-LB, and Gottfried Schatz, Jon Leighton, Andre Goffeau, and Jasper Rine for their generous gifts of some of the antibodies used in this study. We also thank Andy Dancis and Rick Klausner for providing the epitope-tagged *CTR1* gene and pT14, and Hui Zhao and Ann Thering for critical reading of the manuscript.

REFERENCES

1. Lesuisse, E., and Labbe, P. (1989) *J. Gen. Microbiol.* **135,** 257–263
2. Dancis, A., Klausner, R. D., Hinnebusch, A. G., and Barriocanal, J. G. (1990) *Mol. Cell. Biol.* **10,** 2294–2301
3. Eide, D., Davis-Kaplan, S., Jordan, I., Sipe, D., and Kaplan, J. (1992) *J. Biol. Chem.* **267,** 20774–20781
4. Johnson, W., Varner, L., and Poch, M. (1991) *Infect. Immun.* **59,** 2376–2381
5. Evans, S. L., Arceneaux, J. E. L., Byers, B. R., Martin, M. E., and Aranha, H. (1986) *J. Bacteriol.* **168,** 1096–1099
6. Ecker, D. J., and Emery, T. (1983) *J. Bacteriol.* **155,** 616–622
7. Roman, D. G., Dancis, A., Anderson, G. J., and Klausner, R. D. (1993) *Mol. Cell. Biol.* **13,** 4342–4350
8. Römheld, V., and Marschner, H. (1983) *Plant Physiol.* (*Bethesda*) **71,** 949–954
9. Grusak, M. A., Welch, R. M., and Kochian, L. V. (1990) *Plant Physiol.* (*Bethesda*) **94,** 1353–1357
10. Raja, K. B., Simpson, R. J., and Peters, T. J. (1992) *Biochim. Biophys. Acta* **1135,** 141–146
11. Núnez, M. T., Alvarez, X., Smith, M., Tapia, V., and Glass, J. (1994) *Am. J. Physiol.* **267,** C1582–C1588
12. Han, O., Failla, M. L., Hill, A. D., Morris, E. R., and Smith, J. C. (1994) *J. Nutr.* **125,** 1291–1299
13. Jordan, I., and Kaplan, J. (1994) *Biochem. J.* **302,** 875–879
14. Oshiro, S., Nakajima, H., Markello, T., Krasnewich, D., Bernardini, I., and Gahl, W. A. (1993) *J. Biol. Chem.* **268,** 21586–21591
15. Watkins, J. A., Altazan, J. D., Elder, P., Lin, C. Y., Nunez, M. T., Cui, X. X., and Glass, J. (1992) *Biochemistry* **31,** 5820–5830
16. Thorstensen, K., and Romslo, I. (1988) *J. Biol. Chem.* **263,** 8844–8850
17. Nunez, M. T., Escobar, A., Ahumada, A., and Gonzalez-Sepulveda, M. (1992) *J. Biol. Chem.* **267,** 11490–11494
18. Dancis, A., Roman, D. G., Anderson, G. J., Hinnebusch, A. G., and Klausner, R. D. (1992) *Proc. Natl. Acad. Sci. U. S. A.* **89,** 3869–3873
19. Georgatsou, E., and Alexandraki, D. (1994) *Mol. Cell. Biol.* **14,** 3065–3073
20. Askwith, C., Eide, D., Van Ho, A., Bernard, P. S., Li, L., Davis-Kaplan, S., Sipe, D. M., and Kaplan, J. (1994) *Cell* **76,** 403–410
21. Yuan, D. S., Stearman, R., Dancis, A., Dunn, T., Beeler, T., and Klausner, R. D. (1995) *Proc. Natl. Acad. Sci. U. S. A.* **92,** 2632–2636
22. De Silva, D. M., Askwith, C. C., Eide, D., and Kaplan, J. (1995) *J. Biol. Chem.* **270,** 1098–1101
23. Stearman, R., Yuan, D. S., Yamaguchi-Iwai, Y., Klausner, R. D., and Dancis, A. (1996) *Science* **271,** 1552–1557
24. Yamaguchi-Iwai, Y., Dancis, A., and Klausner, R. D. (1995) *EMBO J.* **14,** 1231–1239
25. Yamaguchi-Iwai, Y., Stearman, R., Dancis, A., and Klausner, R. D. (1996) *EMBO J.* **15,** 3377–3384
26. Dix, D. R., Bridgham, J. T., Broderius, M. A., Byersdorfer, C. A., and Eide, D. J. (1994) *J. Biol. Chem.* **269,** 26092–26099
27. Kammler, M., Schon, C., and Hantke, K. (1993) *J. Bacteriol.* **175,** 6212–6219
28. Eide, D., Broderius, M., Fett, J., and Guerinot, M. L. (1996) *Proc. Natl. Acad. Sci. U. S. A.* **93,** 5624–5628
29. Eide, D., and Guarente, L. (1992) *J. Gen. Microbiol.* **138,** 347–354
30. Sambrook, J., Fritsch, E. F., and Maniatis, T. (1989) *Molecular Cloning: A Laboratory Manual*, pp. 1.74–1.84, Cold Spring Harbor Laboratory, Cold Spring Harbor, NY
31. Schiestl, R. H., and Gietz, R. D. (1989) *Curr. Genet.* **16,** 339–346
32. Claros, M. G., and Von Heijne, G. (1994) *Comput. Appl. Biosci.* **10,** 685–686
33. Studier, F. W., Rosenberg, A. H., Dunn, J. J., and Dubendorff, J. W. (1990) *Methods Enzymol.* **185,** 60–89
34. Harlow, E., and Lane, D. (1988) *Antibodies: A Laboratory Manual,* pp.

514–551, Cold Spring Harbor Laboratory, Cold Spring Harbor, NY
35. Yaffe, M. P. (1991) *Methods Enzymol.* **194,** 627–643
36. Kölling, R., and Hollenberg, C. P. (1994) *EMBO J.* **13,** 3261–3271
37. Capieaux, E., Rapin, C., Thines, D., Dupont, Y., and Goffeau, A. (1993) *J. Biol. Chem.* **268,** 21895–21900
38. Wright, R., Basson, M., D'Ari, L., and Rine, J. (1988) *J. Cell Biol.* **107,** 101–114
39. Pringle, J. R., Adams, A. E. M., Drubin, D., and Haarer, B. K. (1991) *Methods Enzymol.* **194,** 565–602
40. Sikorski, R. S., and Heiter, P. (1989) *Genetics* **122,** 19–27
41. Rothstein, R. (1991) *Methods Enzymol.* **194,** 281–301
42. Sipos, L., and Von Heijne, G. (1993) *Eur. J. Biochem.* **213,** 1333–1340
43. Jones, E. W. (1991) *Methods Enzymol.* **194,** 428–453
44. Thomas, T. C., and McNamee, M. G. (1990) *Methods Enzymol.* **182,** 499–520
45. Dancis, A., Yuan, D. S., Haile, D., Askwith, C., Eide, D., Moehle, C., Kaplan, J., and Klausner, R. D. (1994) *Cell* **76,** 393–402
46. Parker, R., Herrick, D., Peltz, S. W., and Jacobson, A. (1991) *Methods Enzymol.* **194,** 415–423
47. Stein, W. D. (1990) *Channels, Carriers, and Pumps. An Introduction to Membrane Transport*, pp. 127–169, Academic Press, San Diego
48. Bennett, W. F., Paoni, N. F., Keyt, B. A., Botstein, D., Jones, A. J. S., Presta, L., Wurm, F. M., and Zoller, M. J. (1991) *J. Biol. Chem.* **266,** 5191–5201
49. Lippard, S. J., and Berg, J. M. (1994) *Principles of Bioinorganic Chemistry*, pp. 21–23, University Science Books, Mill Valley
50. Dougherty, D. A. (1996) *Science* **271,** 163–168
51. Clarke, D. M., Loo, T. W., and MacLennan, D. H. (1990) *J. Biol. Chem.* **265,** 6262–6267
52. Clarke, D. M., Loo, T. W., Inesi, G., and MacLennan, D. H. (1989) *Nature* **339,** 476–478
53. Trikha, J., Theil, E. C., and Allewell, N. M. (1995) *J. Mol. Biol.* **248,** 949–967
54. Heginbotham, L., and Mackinnon, R. (1992) *Neuron* **8,** 483–491